

# Thermal evolution of $\text{ZnCo}_2\text{O}_4$ spinel phase in air

Marco PEITEADO,<sup>†</sup> Amador C. CABALLERO and Darko MAKOVEC\*

Department of Electroceramics, Instituto de Cerámica y Vidrio, CSIC, c/ Kelsen 5, Campus de Cantoblanco. 28049 Madrid, Spain

\*Materials Synthesis Department, Jožef Stefan Institute, Jamova 39, 1000 Ljubljana, Slovenia

**$\text{ZnCo}_2\text{O}_4$  ceramics with a spinel-like structure are versatile functional materials which depending on the synthesis conditions may exhibit magnetic, electric, optical and/or catalytic characteristics. However under air atmosphere, cobalt ions experiment different red-ox processes with temperature, so contrary to many other spinel oxides, a low thermal stability can be expected for this cobaltite spinels. In addition, the final outcome of these transformations will be as well defined by the solid state chemistry of the  $\text{ZnO-Co}_x\text{O}_y$  couple, i.e. by the partial solubility of cobalt in zinc oxide and zinc in the different cobalt oxides. At first the similarity in charge and ionic size suggests the possibility of substitutional solid solution for both the  $\text{Co}^{\text{II}}$  into the  $\text{ZnO}$  wurtzite structure and the  $\text{Zn}^{\text{II}}$  into the  $\text{CoO}$  rock-salt structure. However it has been observed that once the spinel structure collapses, all the zinc diffuses into the rock salt phase.**

©2010 The Ceramic Society of Japan. All rights reserved.

Key-words : Zn-Co ceramics, Spinel, Solid state chemistry

[Received August 13, 2009; Accepted November 19, 2009]

## 1. Introduction

Transition metal oxides with a spinel-like structure are versatile functional ceramics which may exhibit magnetic, electric, optical and catalytic properties. The exceptional physicochemical characteristics of transition metals, like several oxidation and spin states, the similarity in ionic radii and the tendency to occupy the tetrahedral and octahedral sites of the spinel structure, are behind this versatility and as a consequence these compounds find application in a wide spectrum of technological fields.<sup>1)</sup> Zinc cobaltite  $\text{ZnCo}_2\text{O}_4$  is one of these compounds, which has long been used as a ceramic color pigment or dyeing material.<sup>2),3)</sup> Due to its spinel-like structure, with a large capability to form stable and variable solid solutions, zinc cobaltite is also attractive as electrocatalyst for many anode processes such as oxygen evolution and chlorine evolution.<sup>4),5)</sup> Moreover,  $\text{ZnCo}_2\text{O}_4$  has shown a very high lithium storage capacity so it is being considered for next generation of anode materials in lithium ion batteries.<sup>3),6)</sup> In the same way, solid solutions of nominal composition  $\text{Zn}_x\text{Co}_{3-x}\text{O}_4$  exhibit improved adsorbent capabilities so they find application as selective catalysts for oxidation and hydrogenation reactions,<sup>7)</sup> as well as for the monitoring and removal of harmful species such as  $\text{Cl}_2$ ,  $\text{NO}_2$ ,  $\text{CO}_2$  and  $\text{H}_2\text{S}$  among others.<sup>8)-10)</sup> Finally in the last years its magnetic behaviour, either as a single compound or as an impurity phase in the  $\text{Zn}_{1-x}\text{Co}_x\text{O}$  system, is under investigation in the field of room temperature ferromagnetic diluted semiconductors for spintronic applications.<sup>1),11)-15)</sup>

For all these applications an accurate control of the synthesis procedure is entirely required since the distribution of cations in the crystallographic sites of the spinel structure, and hence the overall properties of the compound, sturdily depend on the preparation conditions (temperature, annealing time, atmosphere, cooling conditions, etc...).<sup>1),16),17)</sup> Different synthesis routes have been applied to prepare the  $\text{ZnCo}_2\text{O}_4$  nominal phase and different

stable and/or metastable situations have been successfully obtained.<sup>2),3),6),8),10),15)</sup> However there is one issue which remains confusing, related to the thermal stability and consequently the thermal evolution of this spinel structure in air. Under this atmosphere cobalt ions experiment different red-ox processes with temperature,<sup>18)</sup> so contrary to many other spinel oxides, a low thermal stability can be expected for the cobaltite spinels. According to this, some authors have pointed out that the Zn/Co spinel composition undergoes a thermal decomposition centered at  $930^\circ\text{C}$ ,<sup>8)</sup> or  $1000^\circ\text{C}$ ,<sup>19)</sup> which should be attributed to the reduction of the trivalent cobalt to its divalent state. Using different thermal decomposition methods other authors however suggest that zinc cobaltite is only stable up to  $800^\circ\text{C}$ ; at higher temperatures the structure loses oxygen decomposing into a mixture of  $\text{ZnO}$  and  $\text{CoO}$ .<sup>5),20)</sup> Furthermore it has been reported that when heated in air,  $\text{MCo}_2\text{O}_4$  compounds decompose at temperatures as low as  $400\text{--}600^\circ\text{C}$  forming an MO oxide and a cobalt-enriched spinel phase.<sup>21)</sup>

But in addition to the red-ox processes the final outcome of these transformations strongly depends on the solid state chemistry of the  $\text{ZnO-CoO}_x$  couple, i.e. on the partial solubility of cobalt in zinc oxide and zinc in the different cobalt oxides. This topic has been also analyzed in the literature and different interesting data have been obtained working with hydrothermal techniques,<sup>22)</sup> diffusion couples,<sup>23)</sup> hydrolysis reactions in polyol medium,<sup>24)</sup> spray pyrolysis,<sup>25)</sup> freeze-drying,<sup>26)</sup> or even dip coating.<sup>27)</sup> With all these data in mind, the present contribution faces the analysis of the thermal evolution of the  $\text{ZnCo}_2\text{O}_4$  nominal phase in order to throw some light on the stability of a ceramic material which is finding application in current technologies.

## 2. Experimental

$\text{ZnCo}_2\text{O}_4$  nominal spinel powder was prepared via a single-source crystalline oxalate precursor, which ensures random atomic-scale mixing of the ions involved.<sup>28)</sup> The precursor was obtained by room-temperature co-precipitation with oxalic acid of aqueous solutions of zinc and cobalt acetates,

<sup>†</sup> Corresponding author: M. Peiteado; E-mail: mpeiteado@icv.csic.es

Zn(CH<sub>3</sub>COO)<sub>2</sub>·2H<sub>2</sub>O and Co(CH<sub>3</sub>COO)<sub>2</sub>·4H<sub>2</sub>O. Reagent-grade raw materials (Sigma-Aldrich) were used in all cases. The precipitated oxalate was calcined at 400°C to cleanly decompose it into the corresponding oxide. More details about the synthesis method are described elsewhere.<sup>27)</sup> The calcined powder was pressed into pellets and heat treatments were conducted on a tube furnace under air atmosphere and at temperatures ranging from 650 to 1300°C. At these temperatures the samples were subjected to 48 hours of dwell time and rapidly quenched to freeze them in a high-temperature state.

The composition of the powder after the precipitation process was verified by inductively coupled plasma atomic emission spectroscopy (ICP-AES) on a Thermo Jarrell Ash Atomscan 25 Spectrometer. The thermal evolution of the ZnCo<sub>2</sub>O<sub>4</sub> nominal material was followed by differential thermal analysis and thermogravimetry (DTA–TG) on a Netzsch STA 449 C instrument at a heating rate of 3 K/min in air atmosphere. Characterization of the ground up sintered pellets was carried out by means of X-ray diffraction (XRD) and transmission electron microscopy (TEM). For the XRD profile analyses, step-scanned patterns were collected on a Bruker AXS Endeavor 4 Diffractometer in steps of 0.02° and a counting time of 12 s per step. The lattice parameters were estimated by fitting the powder XRD profiles, using the nonlinear least-squares method. For the TEM investigations the ground up powders were deposited on a copper-grid-supported transparent carbon foil. The samples were examined by a field-emission electron-source high-resolution transmission electron microscope HR-TEM Jeol 2010 F equipped with an EDS microanalysis (LINK ISIS EDS 300).

### 3. Results and discussion

Chemical analysis of the as-precipitated product revealed an atomic Co/Zn ratio of 1.992(1), which matches the nominal ZnCo<sub>2</sub>O<sub>4</sub> formula of the spinel compound. DTA–TG measurements depicted in **Fig. 1** show the thermal evolution in air of this precipitated powder. Three major processes can be observed in both curves. At temperatures below 350–400°C, the DTA curve displays an endothermic peak below 200°C followed by an exothermic signal in the vicinity of 300°C. The first peak is usually attributed to the release of the hydrated water from the oxalate precursor, and according to the preparation conditions a different number of water molecules can be found hydrating the precursor.<sup>29)–31)</sup> In our case the TG calculations reveal two molecules of water hydrating the as-formed oxalate. The second reaction is assumed to stand for the further decomposition of the oxalate. Finally, at higher temperatures one more DTA endothermic peak is observed around 900°C which should be

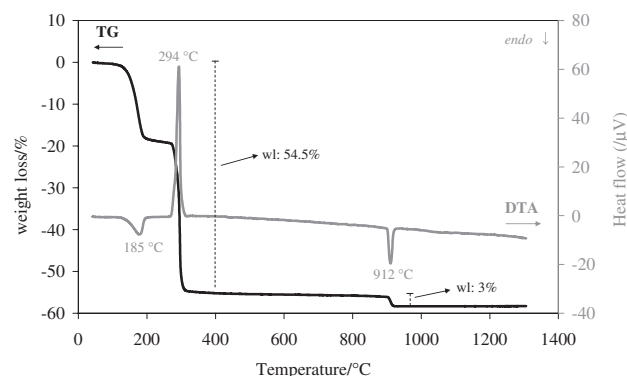


Fig. 1. DTA–TG of the prepared ZnCo<sub>2</sub>O<sub>4</sub> nominal composition.

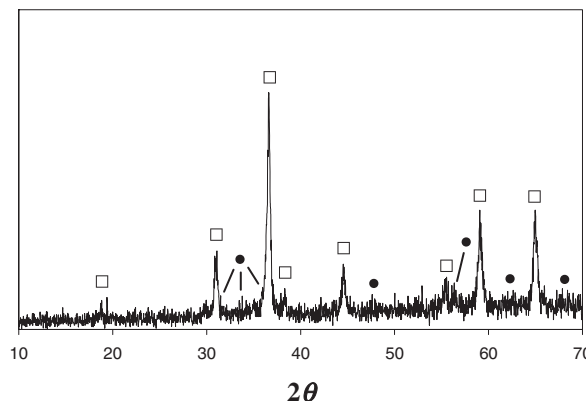


Fig. 2. XRD diffractogram of sample treated at 400°C and air quenched. □ ZnCo<sub>2</sub>O<sub>4</sub> cubic spinel ● ZnO hexagonal zincite.

attributed to the reduction of trivalent cobalt back to its divalent state. Theoretically this process implies a weight loss of 6.5%, but in our case we observe a weight loss of ca. 3% around that temperature (Fig. 1). Such differences should be understood on the fact that when working with oxalates the reduction of Co<sup>III</sup> to Co<sup>II</sup> could start even from the decomposition of the precursor.<sup>21)</sup> Nevertheless if we measure the total weight loss of the overall processes up to 1300°C, an experimental value of ca. 57.5% is obtained which accurately fits the theoretical value of 57.7%.

The thermal evolution indicated by DTA–TG was followed by XRD on powder samples treated at different temperatures. **Figure 2** depicts the XRD diffractogram of the powder treated at 400°C. The observed line broadening evidences a low degree of crystallization, but peaks of the spinel ZnCo<sub>2</sub>O<sub>4</sub> cubic compound are already detected (JCPDS file n° 81-2297). Furthermore, in between the noise of the diffractogram, traces of a secondary phase can be detected as well. These peaks correspond to the zincite ZnO hexagonal compound (JCPDS file n° 36-1451). Initially the presence of this phase could be ascribed to unreacted zinc from the starting precursor composition. However as it was mentioned in the introduction section, some authors have pointed out that already after the decomposition of the oxalate precursor (~400°C), MCo<sub>2</sub>O<sub>4</sub> compounds could be formed by a mixture of an MO oxide and a cobalt-enriched spinel phase.<sup>21)</sup> Actually this situation was already suggested by Robin in a first attempt of equilibrium phase diagram for the ZnO–CoO system at ambient pressure;<sup>32)</sup> according to this diagram, heating the stoichiometric spinel compound above 200°C leads to the formation of ZnO and a spinel phase with a higher content of cobalt.<sup>32)</sup> In our experiments we confirmed such tendency when the temperature was increased. **Figure 3** shows the XRD diffractograms corresponding to the samples treated at 650, 700 and 800°C. As observed the intensity of ZnO peaks gradually increases with temperature, indicating an increased release of zinc from the spinel structure. The explanation to this behaviour should be found in the crystallographic characteristics of the Zn–Co–O spinel. ZnCo<sub>2</sub>O<sub>4</sub> exhibits a normal spinel structure with Zn<sup>II</sup> ions in the tetrahedral sites and Co<sup>III</sup> occupying the octahedral ones. This is attributed to the dominating advantage of placing the d<sup>6</sup> ions in octahedral sites, where adoption of the low-spin configuration gives it a decisively favourable Crystal Field Stabilization Energy.<sup>33)</sup> Accordingly the ionic radii of the cationic species in this spinel structure are 0.60 and 0.545 Å for the Zn<sup>II</sup> and Co<sup>III</sup> ions, respectively.<sup>34)</sup> When temperature is increased Co<sup>III</sup> starts to reduce to Co<sup>II</sup>, a process which as

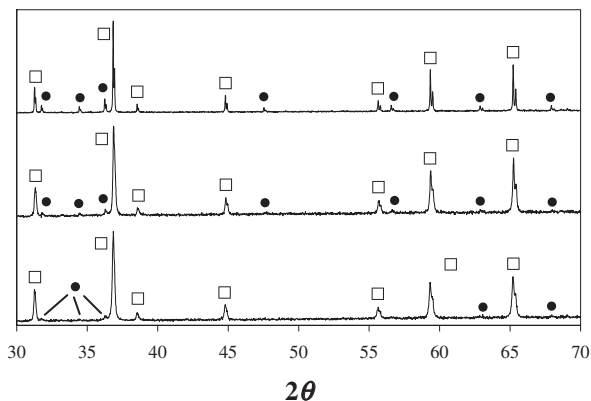


Fig. 3. Down to top, XRD diffractograms of samples treated at 650, 700 and 800°C and air quenched.  $\square$   $\text{ZnCo}_2\text{O}_4$  cubic spinel  $\bullet$  ZnO hexagonal zincite.

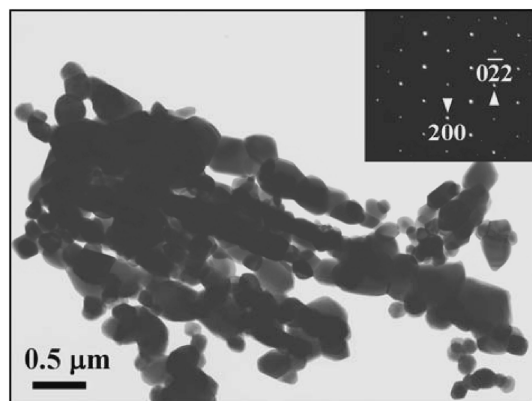


Fig. 4. TEM micrograph of the sample quenched from 650°C. Inset: An electron diffraction pattern taken at individual particle corresponds to the spinel structure along the [011] zone axis.

inferred from DTA–TG gradually proceeds after the decomposition of the oxalate precursor. In four-fold coordination  $\text{Co}^{\text{II}}$  shows an ionic radius of 0.58 Å.<sup>34)</sup> Hence  $\text{Co}^{\text{II}}$  ions can feasibly substitute the  $\text{Zn}^{\text{II}}$  ions in the tetrahedral positions of the spinel arrangement, and in this way zinc is released from the spinel structure leading to the formation of ZnO (Fig. 3). Besides, leaning on the similarity of ionic charge and radii, the substitution of  $\text{Zn}^{\text{II}}$  by  $\text{Co}^{\text{II}}$  ions does not lead to a distortion detectable by XRD of the now cobalt-enriched spinel, explaining why the peaks ascribed to the spinel phase in Fig. 3 does not shift to different angles when the temperature is increased.

TEM image in Fig. 4 corresponds to the sample quenched from 650°C. Particles with relatively uniform size around 100 nm are observed, usually forming large linear agglomerates. Such shape is inherited from the precursor particles and is quite common when working with mixed oxalates.<sup>5),21),35)</sup> Electron diffraction of individual particle matches with spinel structure and quantification of EDS analyses showed a Co/Zn ratio of 2.7+/-0.1, so confirming the Co-enrichment of the spinel compound. Apart from spinel particles, individual particles of ZnO were also present. They look similar to spinel particles and a low content of Co could be also detected in these ZnO particles.

As the reduction of  $\text{Co}^{\text{III}}$  ions progresses, more and more zinc should be released leading subsequently to a more cobalt-enriched spinel. But finally when all the cobalt would be present as  $\text{Co}^{\text{II}}$ , the absence of trivalent ions will lead to the collapse of

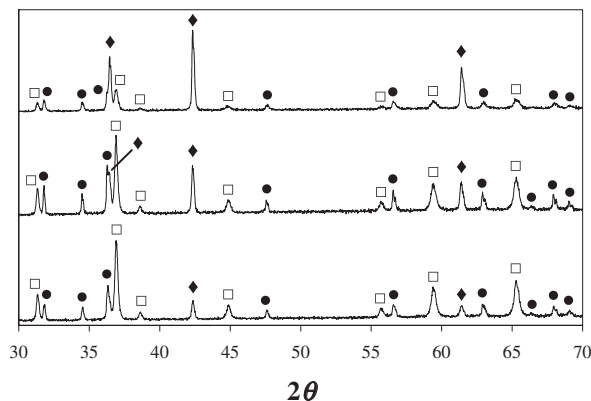


Fig. 5. Down to top, XRD diffractograms of samples treated at 900, 950 and 1000°C and air quenched.  $\square$   $\text{ZnCo}_2\text{O}_4$  cubic spinel,  $\bullet$  ZnO hexagonal zincite,  $\blacklozenge$  CoO cubic rock salt.

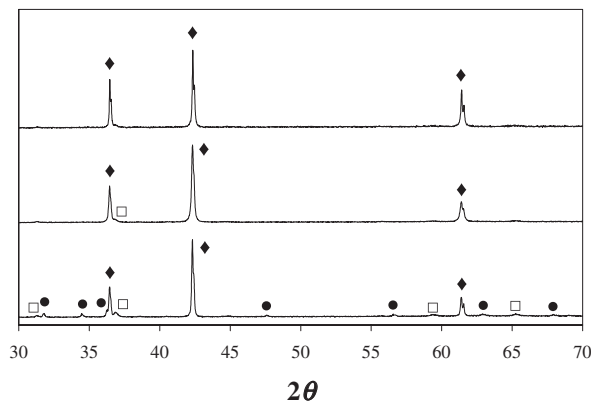


Fig. 6. Down to top, XRD diffractograms of samples treated at 1100, 1200 and 1300°C and air quenched.  $\square$   $\text{ZnCo}_2\text{O}_4$  cubic spinel,  $\bullet$  ZnO hexagonal zincite,  $\blacklozenge$  CoO cubic rock salt.

the spinel structure and a mixture (actually a solid solution) of ZnO and CoO can thus be expected. XRD diffractograms of Fig. 5 corresponding to the samples treated at 900, 950 and 1000°C initially confirm this situation, which as well was predicted by Robin.<sup>32)</sup> As observed in these diffractograms a region is obtained for the temperature range between 900 and 1000°C in which the three components ZnO, spinel, and rock salt CoO coexist. The first peaks of CoO already appear at 900°C, coinciding with the endothermic peak observed in DTA measurements (Fig. 1). With increasing temperature the intensity of the peaks corresponding to CoO gradually increases in spite of a lower intensity of the peaks corresponding to the spinel compound. However, there is one issue which is interesting: the intensity of the peaks ascribed to the ZnO phase also decrease from 950 to 1000°C. Furthermore, the intensity of ZnO peaks continues decreasing when the temperature is increased above 1000°C. Figure 6 depicts the XRD diffractograms of samples treated at 1100, 1200 and 1300°C and around 1200°C, although some minority peaks can be still ascribed to the spinel phase, signals corresponding to ZnO are anymore detected. This situation is clearly indicative of the formation of a stable wide-range solid solution of  $\text{Zn}^{\text{II}}$  ions into CoO, and EDS analysis of the sample fired at 1200°C thus confirmed it. Furthermore, the estimation of the cell parameter of this sample quenched from 1200°C also evidenced the formation of solid solution:  $a = 4.2618 \pm 0.0009 \text{ \AA}$ , significantly larger than that of pure

CoO treated at 1200°C which yields a cell parameter of  $a = 4.2562 \pm 0.0007 \text{ \AA}$ . These results should be interpreted in terms of the crystal chemistry of the involved compounds. As mentioned CoO has the rock-salt structure with Co<sup>II</sup> ions in six-fold coordination. Recent studies indicate that Co<sup>II</sup> ions adopt a high-spin configuration in this arrangement,<sup>36)</sup> which implies an ionic radius of 0.745 Å.<sup>34)</sup> On the other hand ZnO has the wurtzite structure with Zn<sup>II</sup> ions in four-fold coordination and ionic radius of 0.60 Å. The ionic radius of Co<sup>II</sup> decreases to 0.58 Å in tetrahedral coordination and the ionic radius of Zn<sup>II</sup> increases to 0.74 Å when going to octahedral coordination.<sup>34)</sup> At first this similarity in charge and ionic size suggests the possibility of substitutional solid solution for both the Co<sup>II</sup> into the ZnO wurtzite structure and the Zn<sup>II</sup> into the CoO rock-salt structure. However in a previous contribution we have checked that no diffusion of cobalt is ever detected from the rock-salt structure of CoO compound, and temperatures higher than 1200°C should be required to release the Co<sup>II</sup> ions from the rock-salt arrangement.<sup>23)</sup> On the opposite, the diffusion of Zn<sup>II</sup> ions into the rock-salt structure is greatly enhanced above 800°C.<sup>23)</sup> And this is exactly what is observed in the diffractograms of Fig. 6, where all the peaks finally can be ascribed to the CoO phase.

#### 4. Conclusions

The thermal evolution of ZnCo<sub>2</sub>O<sub>4</sub> spinel compound has been analyzed and interpreted in terms of solid state chemistry. The as-formed spinel undergoes several transformations with temperature which are related to the different red-ox processes experimented by cobalt ions under air atmosphere. Initially ZnCo<sub>2</sub>O<sub>4</sub> exhibits a normal spinel structure with Zn<sup>II</sup> ions in the tetrahedral sites and Co<sup>III</sup> occupying the octahedral ones. When temperature is increased Co<sup>III</sup> starts to reduce to Co<sup>II</sup> and these last ions can feasibly substitute the Zn<sup>II</sup> ions in the tetrahedral positions of the spinel arrangement. In this way zinc is released from the spinel structure leading to ZnO and a cobalt-enriched spinel. At higher temperatures when all the cobalt is present as Co<sup>II</sup>, the absence of trivalent ions leads to the collapse of the spinel structure and a mixture of ZnO and CoO should be expected. However whereas the diffusion of Zn<sup>II</sup> ions into the rock-salt structure is greatly enhanced above 800°C, temperatures higher than 1300°C are required to release the Co<sup>II</sup> ions from the rock-salt arrangement. As a consequence once the spinel decomposes the only detected phase is CoO, with all the starting zinc inside the rock salt structure.

**Acknowledgement** This work has been supported by the Ministry of Higher Education, Science and Technology of Slovenia. Also it has been conducted within the CICYT MAT 2007-65857 and CICYT MAT 2007-66845-C02-01 projects. M.P. also acknowledges the Secretaría de Estado de Universidades e Investigación del Ministerio de Ciencia e Innovación (Spain) for the financial support.

#### References

- 1) G. V. Bazuev and O. I. Gyrdasova, *Phys. Status Solidi B*, **245**, 1184–1190 (2008).
- 2) C. Feldmann, *Adv. Funct. Mater.*, **13**, 101–107 (2003).
- 3) C. C. Ai, M. C. Yin, C. W. Wang and J. T. Sun, *J. Mater. Sci.*, **39**, 1077–1079 (2004).
- 4) B. Chi, J. B. Li, X. Z. Yang, H. Lin and N. Wang, *Electrochim. Acta*, **50**, 2059–2064 (2005).
- 5) G. V. Bazuev, O. I. Gyrdasova, I. G. Grigorov and O. V. Koryakova, *Inorg. Mater.*, **41**, 288–292 (2005).
- 6) Y. Sharma, N. Sharma, G. V. S. Rao and B. V. R. Chowdari, *Adv. Funct. Mater.*, **17**, 2855–2861 (2007).
- 7) K. Omata, T. Takada, S. Kasahara and M. Yamada, *Appl. Catal. A Gen.*, **146**, 255–267 (1996).
- 8) T. Baird, K. C. Campbell, P. J. Holliman, R. W. Hoyle, D. Stirling, B. P. Williams and M. Morris, *J. Mater. Chem.*, **7**, 319–330 (1997).
- 9) T. Baird, K. C. Campbell, P. J. Holliman, R. W. Hoyle, M. Huxam, D. Stirling, B. P. Williams and M. Morris, *J. Mater. Chem.*, **9**, 599–605 (1999).
- 10) X. S. Niu, W. P. Du and W. M. Du, *Sens. Actuators B Chem.*, **99**, 405–409 (2004).
- 11) M. S. González-Martínez, J. F. Fernández, F. Rubio-Marcos, I. Lorite, J. L. Costa-Kramer, A. Quesada, M. A. Banares and J. L. G. Fierro, *J. Appl. Phys.*, **103**, 083905 (2008).
- 12) X. F. Wang, R. K. Zheng, Z. W. Liu, H. P. Po, J. B. Xu and S. P. Ringer, *Nanotechnology*, **19**, 455702 (2008).
- 13) Y. L. Liu and J. L. MacManus-Driscoll, *Appl. Phys. Lett.*, **94**, 022503 (2009).
- 14) K. Samanta, P. Bhattacharya, R. S. Katiyar, W. Iwamoto, P. G. Pagliuso and C. Rettori, *Phys. Rev. B*, **73**, 245213 (2006).
- 15) H. J. Kim, I. C. Song, J. H. Sim, H. Kim, D. Kim, Y. E. Ihm and W. K. Choo, *J. Appl. Phys.*, **95**, 7387–7389 (2004).
- 16) J. Ponce, E. Rios, J. L. Rehspringer, G. Poillerat, P. Chartier and J. L. Gautier, *J. Solid State Chem.*, **145**, 23–32 (1999).
- 17) T. Nissinen, Y. Kiros, M. Gasik and M. Lampinen, *Mater. Res. Bull.*, **39**, 1195–1208 (2004).
- 18) C. B. Wang, H. K. Lin and C. W. Tang, *Catal. Lett.*, **94**, 69–74 (2004).
- 19) P. A. Reyes and J. F. Plaza de los Reyes, *Bull. Soc. Chim. Belg.*, **93**, 851–856 (1984).
- 20) N. Deb, *Indian J. Chem. A*, **42**, 506–509 (2003).
- 21) P. Peshev, A. Toshev and G. Gyurov, *Mater. Res. Bull.*, **24**, 33–40 (1989).
- 22) C. H. Bates, W. B. White and R. Roy, *J. Inorg. Nucl. Chem.*, **28**, 397–405 (1966).
- 23) M. Peiteado, D. Makovec, M. Villegas and A. C. Caballero, *J. Solid State Chem.*, **181**, 2456–2461 (2008).
- 24) L. Poul, S. Ammar, N. Jouini, F. Fievet and F. Villain, *Solid State Sci.*, **3**, 31–42 (2001).
- 25) V. Jayaram, J. Rajkumar and B. S. Rani, *J. Am. Ceram. Soc.*, **82**, 473–476 (1999).
- 26) H. Yang and S. Nie, *Mater. Chem. Phys.*, **114**, 279–282 (2009).
- 27) B. B. Straumal, A. A. Mazilkin, S. G. Protasova, A. A. Myatiev, P. B. Straumal and B. Baretzky, *Acta Mater.*, **56**, 6246–6256 (2008).
- 28) A. S. Risbud, N. A. Spaldin, Z. Q. Chen, S. Stemmer and R. Seshadri, *Phys. Rev. B*, **68**, 205202 (2003).
- 29) M. Bouloudenine, N. Viart, S. Colis, J. Kortus and A. Dinia, *Appl. Phys. Lett.*, **87**, 052501 (2005).
- 30) V. Jordanovska, R. Trojko and N. Galesic, *Thermochim. Acta*, **198**, 369–380 (1992).
- 31) X. Wei, D. Chen and W. Tang, *Mater. Chem. Phys.*, **103**, 54–58 (2007).
- 32) J. Robin, in: E. M. Levin, C. R. Robbins, H. F. McMurdie and M. K. Resser (Eds.), "Phase Diagrams for Ceramists," Vol. 1, American Ceramic Society, Columbus, OH (1964) p. 52.
- 33) N. N. Greenwood and A. Earnshaw, "Chemistry of the Elements," Pergamon Press, Oxford, UK (1984) pp. 1290–1326.
- 34) R. D. Shannon, *Acta Crystallogr., Sect. A*, **32**, 751–767 (1976).
- 35) M. Peiteado, A. C. Caballero and D. Makovec, *J. Eur. Ceram. Soc.*, **27**, 3915–3918 (2007).
- 36) S. C. Petitto and M. A. Langell, *Surf. Sci.*, **599**, 27–40 (2005).